

A Three-Dimensionally Oriented Texture for Poly($\alpha,\alpha,\alpha',\alpha'$ -tetrafluoro-*p*-xylylene)

Soo-Young Park,[†] John Blackwell,^{*,†} Sergei N. Chvalun,^{†,‡} Karen A. Mailyan,[‡] Andei V. Pebalk,[‡] and Igor E. Kardash[‡]

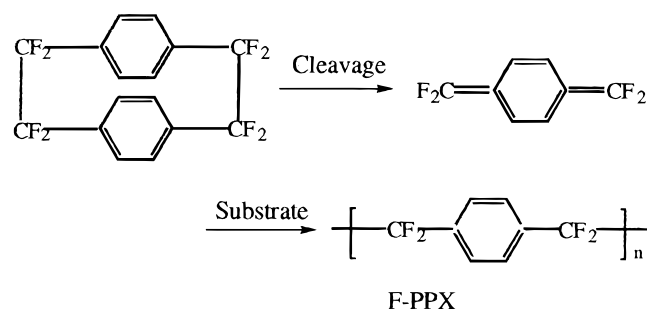
Department of Macromolecular Science, Case Western Reserve University, Cleveland, Ohio 44106-7202, and Karpov Institute of Physical Chemistry, ul Vorontzovo Pole 10, 103064 Moscow, Russia

Received June 30, 1998; Revised Manuscript Received August 13, 1999

ABSTRACT: Films of poly($\alpha,\alpha,\alpha',\alpha'$ -tetrafluoro-*p*-xylylene) prepared by vapor deposition polymerization are highly crystalline and have uniplanar orientation. This orientation is maintained on drawing $\times 10$ at 350 °C, when the chains become aligned parallel to the direction of draw, leading to a texture of three-dimensionally oriented crystals. Thirty-five X-ray reflections are resolved by controlled rotation and tilting of the drawn specimen, and these can be indexed by a triclinic unit cell with dimensions $a = 5.36$ Å, $b = 5.92$ Å, $c = 6.57$ Å (chain axis repeat), $\alpha = 97.0^\circ$, $\beta = 63.1^\circ$, and $\gamma = 73.1^\circ$, containing one monomer unit. Molecular mechanics favors a trans-planar conformation for the $-\text{CF}_2-\text{CF}_2$ linkage which is inclined at 90° to the adjacent phenyl groups, leading to a fiber repeat that is equal to that observed. Packing analyses point to a structure in which the phenyl groups are approximately perpendicular to the ac plane, and this gives good agreement between the observed and calculated structure amplitudes ($R = 0.18$). The crystal structure is similar to that proposed for the α -form of poly(*p*-xylylene), except that the chain separation along the a axis direction is increased due primarily to the presence of the fluorine atoms.

Introduction

Poly(*p*-xylylene) (PPX) is most easily prepared by a vapor deposition polymerization (VDP) of [2,2]paracyclophane, as described by Gorham.¹ Preparation of the analogous fluoro-polymer, poly($\alpha,\alpha,\alpha',\alpha'$ -tetrafluoro-*p*-xylylene) (F-PPX), was first reported by Hertler² in 1963, and its synthesis via the Gorham process is due to Chow et al.,^{3,4} who used 1,1,2,2,9,9,10,10-octafluoro-[2,2]paracyclophane as the precursor in the following scheme:



F-PPX is of interest in view of its potential applications as an interlayer dielectric material in high-speed integrated circuits, since it has an extremely low dielectric constant (< 2.35).^{5–7}

Considerable information is available concerning the structure of the unsubstituted polymer, PPX. Brown and Farhing⁸ reported the existence of two polymorphic crystal structures, designated α - and β -PPX. X-ray and electron diffraction studies by Iwamoto et al.^{9,10} showed that α -PPX is monoclinic with space group $C2/m$; the

unit cell has dimensions $a = 5.92$ Å, $b = 10.64$ Å, $c = 6.55$ Å, and $\beta = 134.7^\circ$ and contains two monomer units. Isoda et al.¹¹ reported that the β -form has a large trigonal unit cell containing 16 monomers, with dimensions $a = b = 20.52$ Å, $c = 6.55$ Å, $\gamma = 120^\circ$, and space group $P3$. Note that the fiber repeat is the same for the two forms: the probable chain conformation has planar, all-trans $-\text{CH}_2-\text{CH}_2-$ groups that are inclined at 90° to the adjacent phenyl rings.^{10,12}

The crystallinity and texture of PPX films, and hence their mechanical properties, are very dependent on the synthesis conditions,^{12–15} notably the sublimation and deposition temperatures. The latter determines the rate of sorption, polymerization, and crystallization of the growing polymer chain. For example, increasing the substrate temperature from -45 to 30 °C resulted in an increase in crystallinity from 35 to 66% for material sublimed at 120 °C. However, PPX deposited at the lower substrate temperature had a more uniplanar texture: the azimuthal half-width of the $\bar{2}01$ reflection was 25.8° when the substrate was -30 °C but increased to 39.6° at 10 °C. Increasing the sublimation temperature from 120 to 160 °C resulted in a decrease in both the crystallinity and orientation of the films.

The films could be drawn up to $\times 40$ at 350 °C, and the drawn films retained their uniplanar orientation, but with conversion to the β -form. The drawn β -PPX films have a doubly oriented, single-crystal-like texture: the c axis (chain axis) is parallel to the direction of draw, and the a and b axes are preferentially parallel and perpendicular to the plane of the film, respectively.¹⁵ The proposed structures for α - and β -PPX are based on the electron diffraction pattern of single crystals.^{10,11,16–18} X-ray intensity data from doubly oriented specimens have not been utilized for structure analysis.

[†] Case Western Reserve University.

[‡] Karpov Institute of Physical Chemistry.

* To whom correspondence should be addressed.

In the present paper, we will address the oriented texture of drawn films of F-PPX produced by the VDP process. The X-ray intensity data for these specimens have also been used to analyze the crystal structure.

Experimental Section

Poly($\alpha,\alpha,\alpha',\alpha'$ -tetrafluoro-*p*-xylylene) was prepared from 1,1,2,2,9,9,10,10-octafluoro-2,2-paracyclophane by the VDP process. 1,1,2,2,9,9,10,10-Octafluoro-2,2-paracyclophane was synthesized as described by Glechkina et al.¹⁹ The VDP process was carried out using equipment similar to that described by Mailyan et al.¹³ sublimation at 120–125 °C, pyrolysis at 740–750 °C, and deposition on a polished glass substrate at –20 °C at a pressure (before sublimation) of $\sim 5 \times 10^{-3}$ mmHg. The resultant films, which were transparent, tough, and 10–12 μm thick, were peeled from the substrates. As-deposited films were annealed for 30 min at 500 °C. Note that the film strength and toughness were maintained even after annealing at 500 °C. The films were drawn (to a maximum of) $\times 10$ in an oven at 350 °C and annealed at 450 °C for 30 min. The density was measured by flotation in tetrachloroethylene and 1,2-dibromoethane, which are miscible nonsolvents.

Wide-angle X-ray diffraction patterns were recorded on film using Ni-filtered Cu K α radiation, with the beam aligned (a) parallel to the draw direction (designated the OD pattern), (b) normal to the film surface (the ND pattern), and (c) perpendicular to both drawing and normal directions (the TD pattern). Resolution of the hkl reflections in the three-dimensional scattering data was achieved using a Siemens Hi-Star area detector. The film was arranged with the draw direction perpendicular to the beam and tilted by the angle ω equal to the Bragg angle for each layer line, after which it was rotated through the angle ϕ in 10° increments about the draw direction ($\phi = 0^\circ$ for ND direction). The wide angle scattering data perpendicular to the draw direction were also recorded as a $\theta/2\theta$ scan on a Philips PN 3550/10 diffractometer operating in the transmission mode.

The intensity of each reflection was determined by integration (over the entire area of the reflection) after the subtraction of the background scattering and was corrected for differences in effective film thickness due to tilt and rotation as described by Alexander.²⁰ The rotation angle ϕ_i for the intensity maximum for each hkl reflection was determined by interpolation.

Following correction for Lorenz and polarization effects, structure amplitudes, $|F_o(hkl)|$, for 35 observed reflections were derived from the three-dimensional intensity data. Control of ϕ allowed resolution of 10 reflections that would be overlapped in a fiber diagram. However, since the data on different layer lines were collected separately, normalization was necessary. This was done on the basis of the intensities recorded for a specimen with fiber orientation created by rolling a film around the draw direction. The diameter of the rolled film was less than that of the X-ray beam (collimator diameter 0.3 mm). The fiber diagram contained 30 reflections, 13 of which were overlapped and multiply indexed.

A measure of the perfection of the planar texture was derived from the azimuthal half-width of the 010 reflection ($d = 5.4$ Å) in data recorded using the area detector, with the beam parallel to the draw direction (OD pattern). Similarly, an estimate of the axial orientation was obtained from data recorded with the beam normal to the film surface (ND pattern).

Molecular mechanics modeling was performed using the SYBYL software package (Tripos Inc.). Partial charges were calculated using the Gasteiger and Huckel method. The potential energy was computed as the sum of the contribution due to van der Waals, electrostatic forces, distortions of the bond lengths, bond angles, torsional angles, and the effects of out-of-plane bending. The optimum bond length and angles were as follows: C–C(aliphatic) = 1.55 Å, C(aliphatic)–C(aromatic) = 1.53 Å, C–C(aromatic) = 1.40 Å, C–F = 1.36 Å, C–C–C(aliphatic) = F–C–C = F–C–F = 109.5°; all angles

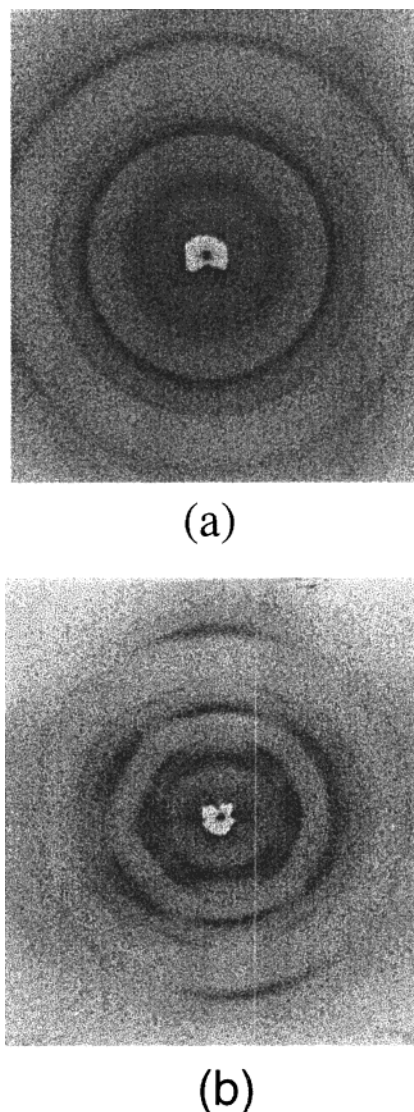
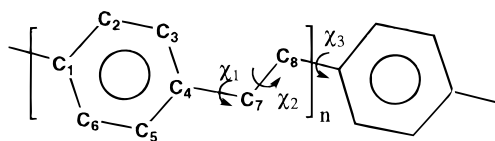


Figure 1. Wide-angle X-ray patterns of the as-deposited film of F-PPX annealed at 500 °C for 30 min with (a) beam perpendicular to the film surface and (b) beam parallel to the film surface (the plane of film surface is vertical).

in the phenylene ring were 120°. The chain conformation depends primarily on torsion angles χ_1 , χ_2 , and χ_3 defined below:



0° for all three torsion angles was for the *cis* position relative to the carbon atoms, and a positive angle corresponded to anticlockwise rotation.

In the packing models, the setting angle ξ for a rigid chain was defined as the rotation about the axis passing through the center of the C7–C8 bonds; $\xi = 0^\circ$ was when the projection of C7–C8 coincides with the *a* axis. In the packing analysis, energy minimization was performed for a 7×7 array of chains, each containing nine monomer units, based on the proposed unit cell dimension. In the starting model, the chain conformation was $\chi_1 = 90^\circ$, $\chi_2 = 180^\circ$, $\chi_3 = -90^\circ$, and $\xi = 90^\circ$. After minimization, the energy was computed for the central seven chains.

The calculated structure amplitudes, $|F_c(hkl)|$, for the proposed structure were calculated using Cerius software. The

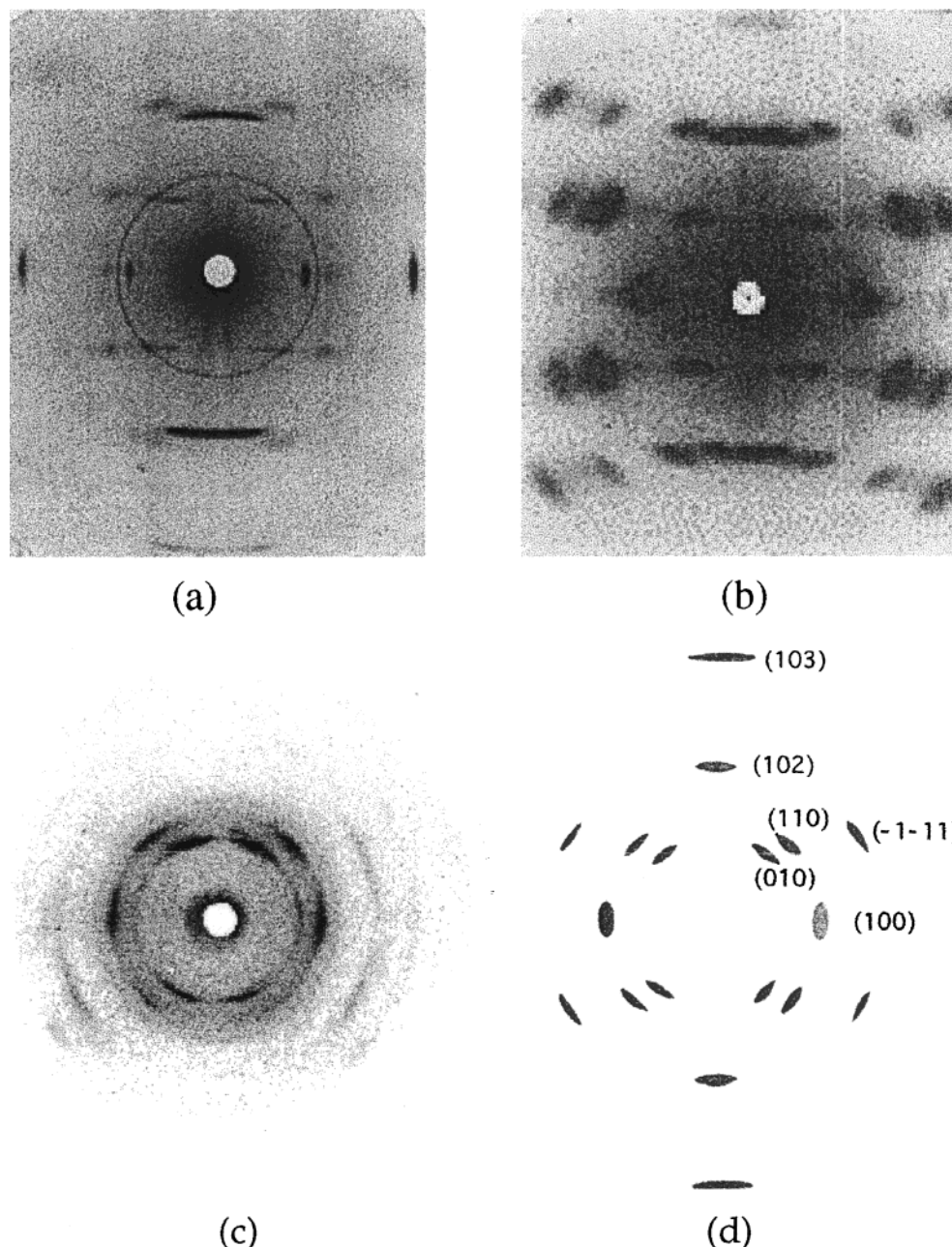


Figure 2. Wide-angle X-ray patterns of the drawn and annealed film of F-PPX with (a) beam along the ND direction, (b) beam along the TD direction, (c) beam along the OD direction (plane of film surface is vertical), and (d) schematic of (c) showing the hkl indices.

crystallographic R value was determined as the sum of the normalized differences between the observed and calculated structural amplitudes:

$$R = \frac{\sum ||F_o(hkl)| - |F_c(hkl)||}{\sum |F_o(hkl)|}$$

Reflections that were predicted within the region of the observed data but were too weak to be observed were included in the $|F_o(hkl)|$ data by assigning intensities of half the threshold detectable intensity.

Results and Discussion

X-ray Diffraction. Figure 1 shows the wide-angle X-ray patterns of the annealed, as-deposited film recorded with the beam (a) perpendicular and (b) parallel to the film surface. Figure 1a contains a series of

isotropic rings; in Figure 1b the data are broken into arcs with the same d spacings. The strong peak at $d = 4.4$ Å in Figure 1b occurs on the equator and derives from planes that are approximately parallel to the film surface. Two broad peaks are observed close to the meridian, at $d = 3.21$ and 2.15 Å. Thus, the data are indicative of a planar texture, which is a recognized characteristic of vapor deposition polymerization.^{9,14} The wide-angle X-ray patterns of the as-deposited unannealed film showed that this also has a planar texture, but the observed reflections were broader and fewer in number. The improvement obtained on annealing occurs with little change of the d spacings and corresponds to an increase in crystallite size and perfection.

Figure 2 shows the ND, TD, and OD wide-angle X-ray patterns of a drawn annealed film, recorded with the beam along the normal, transverse, and draw directions.

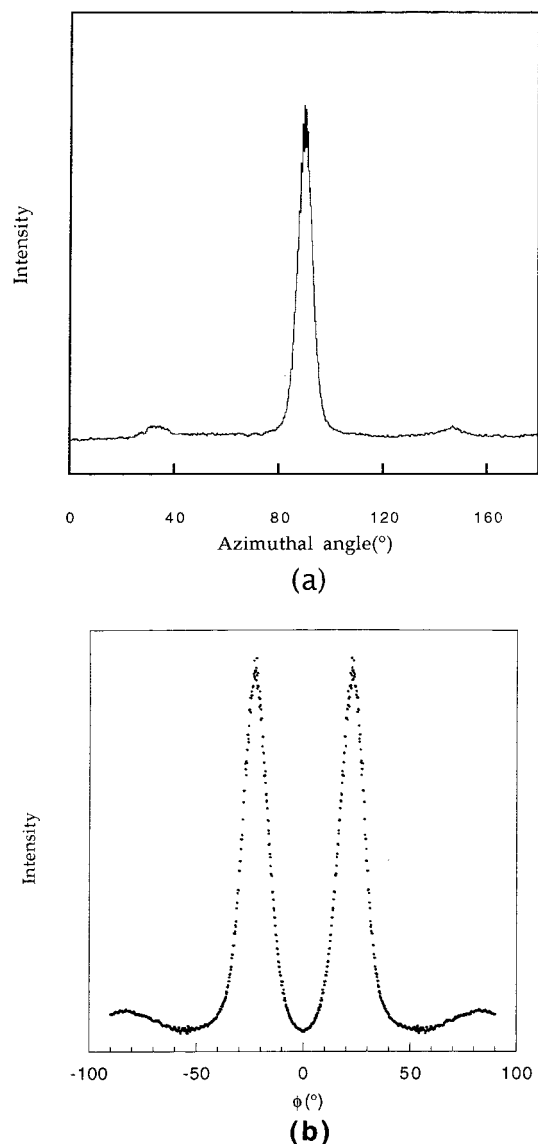


Figure 3. Azimuthal scan of the Bragg peak at $d = 5.4$ Å in (a) the ND pattern and (b) the OD pattern.

Distinct layer lines at orders of 6.57 Å occur perpendicular to the draw direction in both the ND and TD patterns. A azimuthal scan of the reflection at $d = 5.41$ Å is shown in Figure 3a. The half-width is approximately 5.6° , indicating a high degree of axial orientation. Reflections close to meridian are resolved at $d = 3.21$ and 2.15 Å on the second and third layer lines, respectively. These match the d spacings for the broad reflections observed in Figure 1b and originate from planes that are nearly perpendicular to the chain axis.

The data in Figure 2a,b contain many reflections with the same d spacings but with very different relative intensities, pointing to a highly oriented texture. For example, the first equatorial peak at $d = 5.41$ Å is much stronger in the ND pattern than in the TD pattern. In contrast, the second equatorial peak at $d = 4.41$ Å is much stronger in the TD pattern than in the ND pattern. These differences indicate that the planar texture of the as-deposited film persists after drawing and annealing, i.e., the drawn film has double orientation, similar to that occurs in some semicrystalline polymer films that have been pressed and drawn.^{21,22} However, the double orientation in the vapor-deposited films is much more extensive than can be achieved in

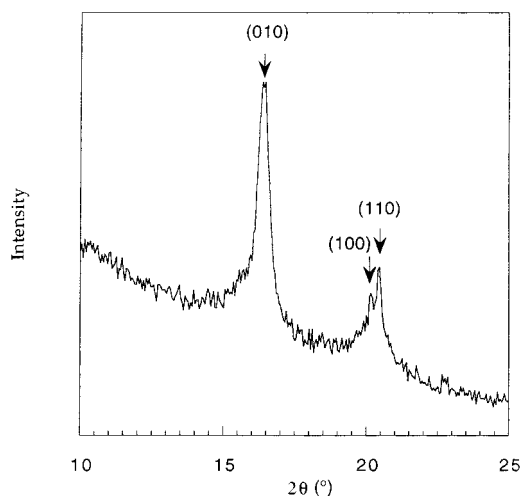


Figure 4. A $2\theta/\theta$ diffractometer scan of the drawn and annealed film of F-PPX, corresponding to along the equatorial direction of the ND pattern.

the latter system, as can be seen from the OD pattern where we observe a number of arced reflections. If the specimen had uniaxial orientation, these would be rings of uniform intensity. Figure 3b shows an azimuthal scan through the first Bragg peak at $d = 5.41$ Å ($\phi = 23^\circ$), for which the half-width is 13° , pointing to a high degree of double orientation. Typical half-widths for doubly oriented pressed polymer films are 30 – 40° .^{21,22} Thus, the texture of the drawn film is similar to that of single crystal.

Figure 4 shows the diffractometer scan of an oriented film along the equatorial direction of ND pattern. The peak in the region of $2\theta = 21^\circ$ is seen to be split into two components at $d = 4.41$ and 4.35 Å. In the OD pattern, these reflections are well separated at $\phi = 90^\circ$ and 42° , respectively: we observe two sets of data that are mirror images of each other, since the doubly oriented film contains crystals in two orientations. Other than this, the texture of the drawn F-PPX film is similar to that of a single crystal.

Unit Cell Determination. On the basis of the above X-ray data, we can conclude that F-PPX has triclinic symmetry, because there are no row lines in the ND and TD patterns. A fiber repeat of $c = 6.57 \pm 0.02$ Å can be determined from layer line separation in the ND and TD patterns. The OD pattern relates to the projection of the structure perpendicular to the chain axis and defines the reciprocal lattice vectors \mathbf{a}^* and \mathbf{b}^* . A reasonable indexing scheme would be to take the strong equatorial reflection at $d = 4.41$ Å as 100 and assign those at $d = 4.35$ and 5.41 Å as 010 and 110, respectively, as shown in Figure 2d. So a^* and b^* are $1/4.41$ Å⁻¹ and $1/5.41$ Å⁻¹; the angle $\gamma^* = 113.0^\circ$ is determined from the d spacings of the 100, 010, and 110 reflections and confirmed by disposition of these reflections on the OD pattern.

The only remaining unknown is c^* , which requires indexing of the first two reflections on the first layer line, to specify their reciprocal lattice coordinates $[x, y, 1/6.57]$. Figure 5 shows the projection of these $hk1$ lattice points on the $hk0$ base plane of the reciprocal lattice. The vector between these two lattice points has the same magnitude and direction as that between the origin and the 100 point. This strongly suggests that the first two peaks have the same k index and that their h indices differ by 1. Thus, the first and second peaks

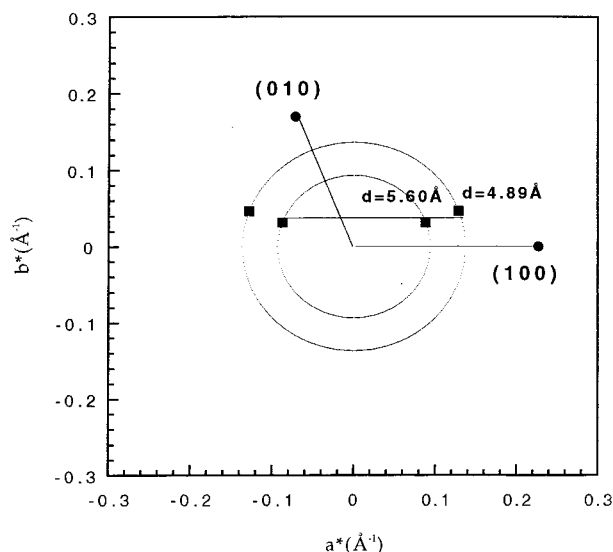


Figure 5. Projection of the first two hkl lattice points on the $hk0$ base plane of the reciprocal lattice: ■, hkl ; ●, $hk0$.

on the first layer line can be indexed as 001 and 101, respectively. The a^* , b^* , and c^* vectors in reciprocal lattice are now defined, and the unit cell parameters of F-PPX are $a = 5.36 \pm 0.02$ Å, $b = 5.92 \pm 0.02$ Å, $c = 6.57 \pm 0.02$ Å, $\alpha = 97.0 \pm 0.2^\circ$, $\beta = 63.1 \pm 0.2^\circ$, and $\gamma = 73.1 \pm 0.2^\circ$. If the unit cell contains one monomer unit, the density of the crystalline structure is 1.71 g/cm³, which compares very favorably with the observed density of 1.69 g/cm³ for a highly crystalline polymer. The observed and calculated d spacings and assigned hkl indices are given in Table 1 and are seen to be in good agreement.

Figure 6 shows intensity scans along the equator and layer lines 1–3 at 10° increments of rotation ϕ about the draw direction ($f = 0$ and $\phi = 90^\circ$ correspond to the ND and TD orientation, respectively). The value of ϕ for each maximum was obtained by interpolation. These data are given as $\phi_o(hkl)$ in Table 1 and are seen to compare very well with the predicted angles, $\phi_c(hkl)$. The values for $\phi_c(hkl)$ are derived for the reciprocal lattice oriented as defined by the observed texture; those for $\phi_o(hkl)$ have been corrected for curvature of the Ewald sphere. (The experimentally measured values before correction are given in Table 1 in parentheses.) As an example of the good agreement, the strong 010 reflection at $\phi_o = 30^\circ$ is predicted to occur at $\phi_c = 31^\circ$; the 100 and 110 reflections are clearly separated at $\phi_o = 50^\circ$ and 90° , respectively, and match the predicted values of ϕ_c of 48° and 90° . Note that the sign of ϕ cannot be determined because the reciprocal lattice point and its mirror image are superimposed.

Model Building. The observed fiber repeat of $c = 6.57 \pm 0.02$ Å is within experimental error of that for PPX ($c = 6.55$ Å) and strongly suggests that the chain conformations are very similar, despite the replacement of the hydrogens by fluorine atoms. Molecular mechanics modeling shows that the minimum-energy conformation for the isolated F-PPX chain has a trans-planar tetrafluoroethylene unit ($\chi_2 = 0^\circ$) and that the plane of the “zigzag” is perpendicular to the plane of the phenylene ring ($\chi_1 = 90^\circ$ and $\chi_3 = -90^\circ$). This chain has one monomer unit in a repeat of $c = 6.57$ Å, which is the same as that observed, and is in accord with the predictions for PPX.^{6–8}

Table 1. Comparison of the Observed and Calculated d spacings, Azimuthal Angles (Φ) for the Bragg Reflections, and Their Observed and Calculated Structure Amplitudes

h	k	l	d_o (Å)	d_c (Å)	ϕ_o (deg) ^a	ϕ_c (deg)	F_o	F_c
0	1	0	5.41 ± 0.02	5.41	21 (29)	–23	8.96	8.50
1	0	0	4.41 ± 0.02	4.41	90 (90)	90	4.89	6.22
1	1	0	4.35 ± 0.02	4.35	39 (49)	42	6.66	5.96
0	2	0	2.70 ± 0.03	2.70	22 (39)	23	3.47	4.07
0	0	1	5.59 ± 0.03	5.59	78 (82)	78	2.75	2.37
1	0	1	4.89 ± 0.03	4.89	74 (80)	–82	2.23	2.67
1	1	1	3.8 ± 0.1	3.99	10 (20)	23	1.73	2.42
0	1	1	3.46 ± 0.04	{3.45	49 (60)	{–47	1.62	1.99
1	1	1		{3.35		{–48		
1	1	1	3.03 ± 0.03	3.06	54 (67)	53	7.04	6.87
1	0	1	2.82 ± 0.03	2.82	90 (90)	87	2.11	3.18
2	1	1	2.59 ± 0.04	2.64	49 (65)	62	2.48	3.25
1	1	1	2.14 ± 0.03	{2.17	60 (80)	{–67	3.46	3.32
2	1	1		{2.06		{–66		
2	1	1	1.89 ± 0.03	1.92	57 (80)	68	2.82	2.18
1	0	2	3.21 ± 0.02	3.23	52 (55)	–49	9.23	9.43
1	1	2	2.87 ± 0.03	2.84	32 (40)	–29	2.39	2.37
2	0	2	2.42 ± 0.04	{2.44	62 (75)	{–82	2.16	2.27
				{2.39		{56		
1	2	2	2.16 ± 0.04	2.13	22 (38)	–26	2.23	2.67
1	1	2	2.09 ± 0.04	2.11	54 (71)	58	3.53	2.83
1	2	2	1.99 ± 0.03	{2.02	27 (45)	{–18	2.48	3.17
1	2	2		{1.98		{35		
1	0	2	1.96 ± 0.03	1.95	90 (90)	85	1.16	1.08
3	1	2	1.72 ± 0.04	1.78	57 (80)	73	1.98	2.24
1	3	2	1.65 ± 0.04	1.62	15 (40)	–25	1.14	1.65
1	3	2	1.54 ± 0.04	1.54	13 (40)	–20	1.52	1.16
3	1	2	1.51 ± 0.04	1.52	62 (90)	70	1.54	0.82
1	1	3	2.15 ± 0.03	{2.12	31 (35)	{–6	10.2	10
1	0	3		{2.16		{41		
2	0	3	2.01 ± 0.02	2.03	55 (64)	–73	3.52	3.77
2	1	3	1.88 ± 0.03	{1.92	57 (70)	{43	1.62	1.91
2	1	3		{1.88		{–48		
2	2	3	1.88 ± 0.04	1.86	7 (20)	6.8	1.11	0.5
0	1	3	1.63 ± 0.03	1.62	45 (65)	–72	1.90	1.13
1	2	3	1.56 ± 0.03	{1.57	8 (30)	{–34	2.25	1.94
0	–3	3		{1.55		{6		
2	0	4	1.60 ± 0.03	{1.61	38 (45)	{–49	3.70	3.13
2	1	4		{1.57		{–33		
0	1	4	1.46 ± 0.03	1.46	50 (66)	50	4.35	3.39
0	2	4	1.43 ± 0.03	1.43	22 (40)	28	2.17	1.60
0	3	4	1.27 ± 0.04	1.31	4 (70)	–14	1.11	1.12
2	0	5 ^b	1.31 ± 0.02	1.30			4.35	2.80

^a Data in parentheses represent experimentally measured values. ^b Measured from the meridional diffractometer scan.

Inspection of the unit cell shows that the chain will pack with the phenyl rings approximately perpendicular to the ac plane. Figure 7 is a plot of the potential energy for structures in which the setting angle, ξ , was varied in 1° increments from 80° to 100° . Minimum energy was at $\xi = 91^\circ$, and this setting was used to construct the model as shown in Figure 8. Compared to $\xi = 90^\circ$, the energy difference is negligible, but if we use the alternative two-chain unit cell (dotted lines in Figure 8a), the angle between a and b' (γ') is 91° .

After energy minimization of a 7×7 array of chain of nine monomers, the chain conformation of the center chain showed little change ($\chi_1 = 89.5^\circ$, $\chi_2 = 180^\circ$, $\chi_3 = -89.5^\circ$, $\xi = 90.5^\circ$). The energy of the central seven chains, i.e., the center chain and its six immediate neighbors, fell from -1.71 to -1.76 kcal/mol of monomer. Thus, it appears that the crystal structure contains chains with a conformation very similar to that predicted for the isolated molecule.

The ultimate test for a correct structure is the agreement between the observed and calculated intensities. Figure 9 shows a plot of the crystallographic R

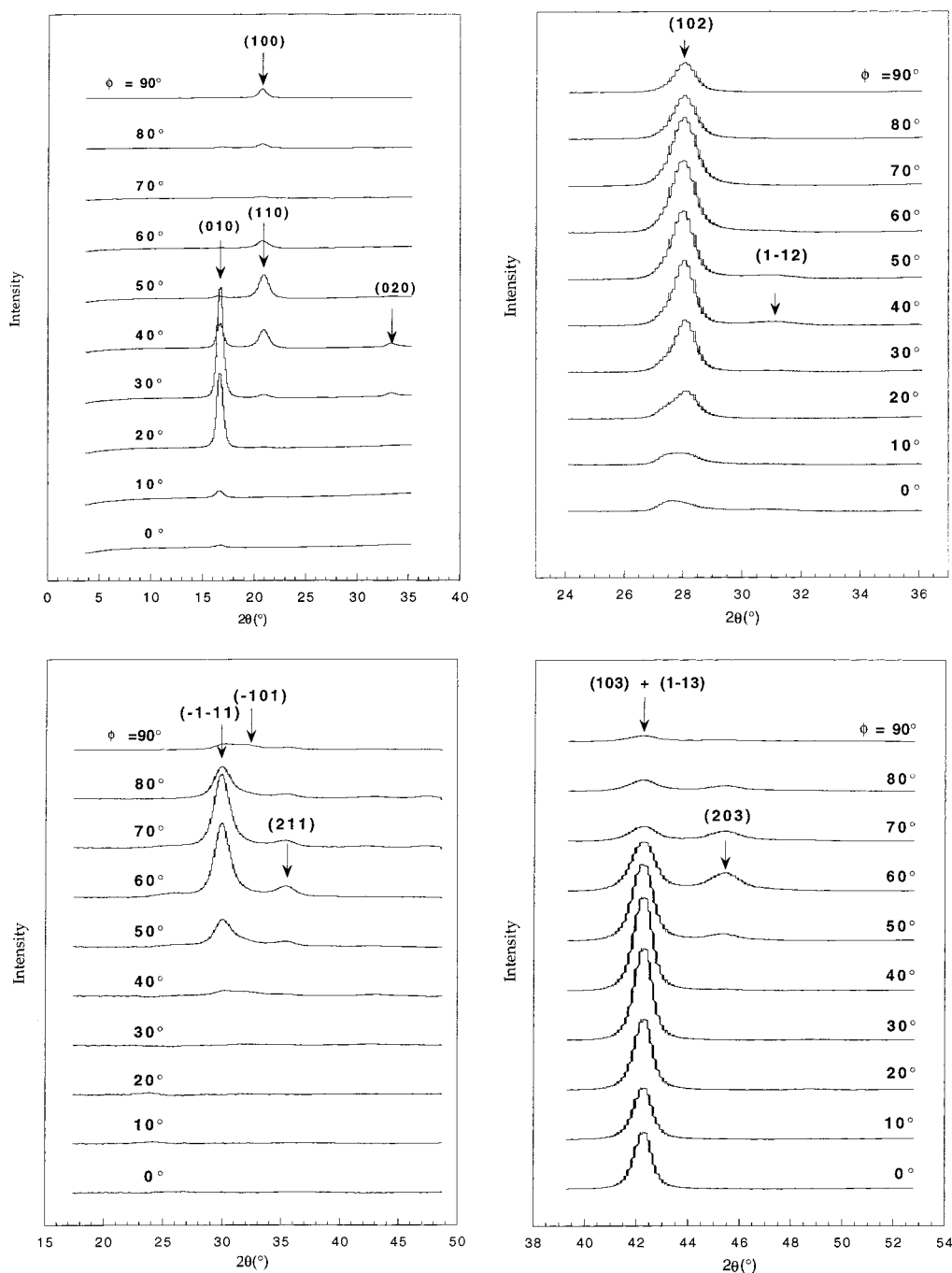


Figure 6. Layer scans of the area detector frame along equatorial, first, second, and third layer lines with $\phi = 0^\circ$ – 90° in 10° increments: (a) the equatorial scan with $2\theta/\theta$ condition = 0° ; (b) the first layer line scan with $2\theta/\theta$ condition = 6.57 \AA ; (c) the second layer line scan with $2\theta/\theta$ condition = $6.57/2 \text{ \AA}$; (d) the third layer line scan with $2\theta/\theta$ condition = $6.57/3 \text{ \AA}$.

value against rotation angle, ξ , for models based on the predicted unit cell. R is strongly dependent on ξ and has a minimum value of 0.18 in the region of $\xi = 90^\circ$, coincident with the minimum energy. Such a low value of R represents excellent agreement for a model that is not fully refined and would be expected to fall a little further if that were to be done.

Comparison with the Structure of PPX. The ab projection of the structure of F-PPX in Figure 8 is very similar to that of α -PPX, which has monoclinic symmetry ($\beta \neq 90^\circ$). The 16% increase in unit cell volume for F-PPX is due to the presence of the larger fluorine atoms. The unit cell is dilated mainly along a , which increases from 4.21 \AA (α -PPX) to 4.78 \AA (F-PPX), and it can be seen that the C–F bonds point approximately

in that direction. The chain staggering of F-PPX in the ab projection is much smaller than that in α -PPX as shown in Figure 8c (-2.08 \AA in α -PPX vs -0.726 \AA in F-PPX). The chain staggering occurs primarily in the ac projection, as shown in Figure 8b, and is essentially the same as in α -PPX (2.43 \AA in F-PPX vs 2.39 \AA in PPX).

However, there is a major difference between the two polymers in terms of the orientation of the molecules during deposition, as shown in Figure 10. In F-PPX, the (100) plane is parallel to the film surface, and the planes of the phenylene groups are inclined at 23° thereto (Figure 10a). In contrast, in the as-polymerized film of α -PPX, the (010) plane is parallel to substrate surface,^{9,14} such that the phenylene rings are perpendicular

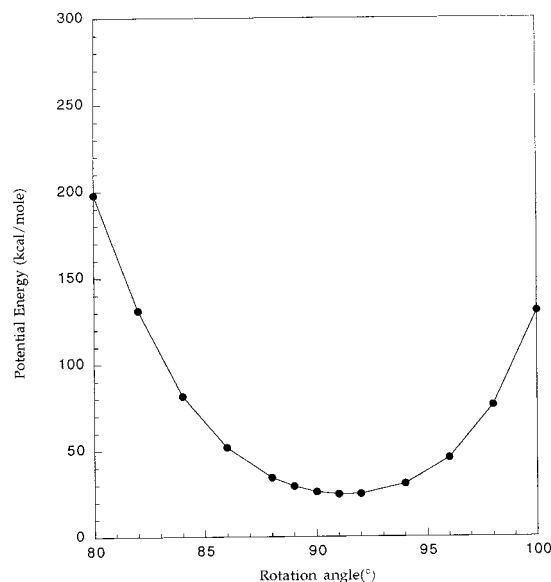


Figure 7. Potential energy of five chains in Figure 8a plotted against ξ .

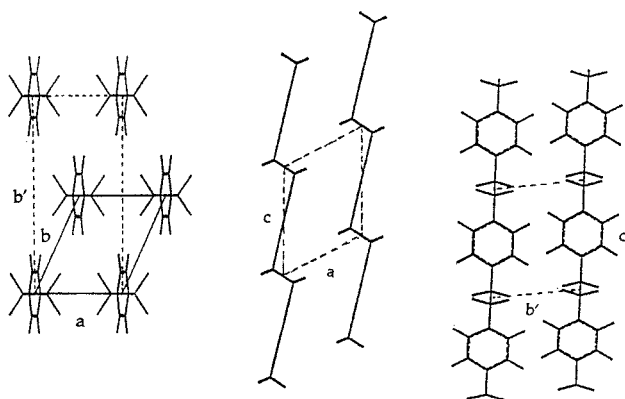


Figure 8. Proposed crystal structure of F-PPX: (a, left) *ab* projection, (b, middle) *ac* projection, and (c, right) *bc* projection.

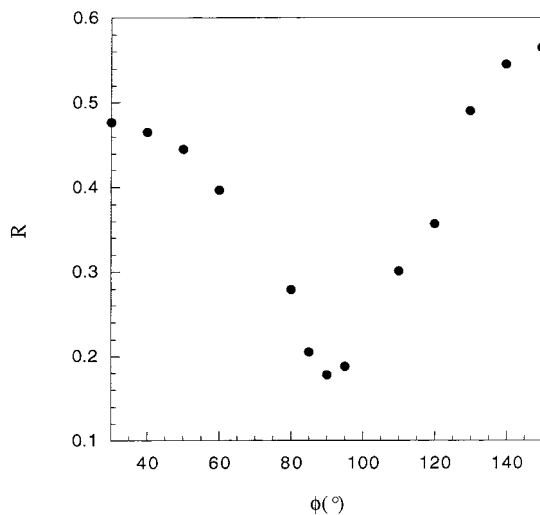


Figure 9. Plot of *R* value against ξ .

to the surface (Figure 10b). This difference in the orientation of aromatic units may be explained by the lower packing density in the 010 plane in the structure of F-PPX, as a result of dilation along *a* axis. The substitution of fluorine atoms also increases the polarity of chain, which probably enhances the interaction

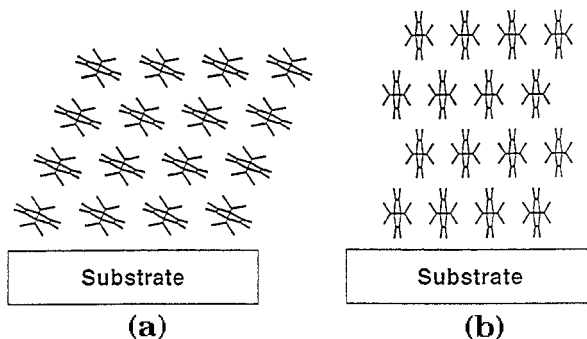


Figure 10. Deposition of (a) F-PPX and (b) α -PPX on the substrate (projection along the chain axis direction).

between the substrate and the growing polymer. Other possible explanations include the higher rigidity of the F-PPX chain and the higher glass transition temperature (>100 °C compared to ~ 15 °C for PPX).²³

Conclusions

The F-PPX film made by the VDP process has a well-developed planar texture. This planar texture is maintained during drawing at 350 °C, when a high degree of chain orientation is developed. The resultant film has a doubly oriented, single-crystal texture, with the 100 plane parallel to the plane of the film and the chain axis parallel to the draw direction. The three-dimensional wide-angle X-ray data show that the unit cell of F-PPX is triclinic, with dimensions $a = 5.36$ Å, $b = 5.92$ Å, $c = 6.57$ Å, $\alpha = 97.0^\circ$, $\beta = 63.1^\circ$, and $\gamma = 73.1^\circ$, and contains one monomer unit. The observed and calculated *d* spacings are in good agreement, and the proposed unit cell dimensions also predict the observed azimuthal angles for the intensity maxima, as defined by the three-dimensional texture.

Molecular mechanics modeling predicts a minimum-energy conformation in which the trans-planar "zigzag" $-\text{CF}_2-\text{CF}_2-$ unit is inclined perpendicular to the phenylene group. Packing such a chain in the proposed lattice leads to excellent agreement between the observed and calculated structure amplitudes ($R = 0.18$). The *ab* projection of the crystal structure is very similar to that observed for the α -form of PPX. However, the structure of F-PPX is more dilated in the *a* axis direction as compared to α -PPX, due primarily to the presence of the larger fluorine atoms. The plane of phenylene rings of F-PPX is perpendicular to the *ac* plane and tilted 23° out of the 100 plane. In this regard the texture is different from that reported for PPX, where the phenylene units are normal to the 100 plane.

References and Notes

- (1) Gorham, W. F. *J. Polym. Sci., Part A-1* **1966**, 4 (12), 3027.
- (2) Hertler, W. R. *J. Org. Chem.* **1963**, 28, 2877.
- (3) Chow, S. W.; Pilato, L. A.; Wheelwright, W. L. *J. Org. Chem.* **1970**, 35, 20.
- (4) Chow, S. W.; Loeb, W. E.; White, C. E. *J. Appl. Polym. Sci.* **1969**, 13 (11), 2325.
- (5) Dabral, S.; Zhang, X.; Wu, X. M.; Yang, G.-R.; You, L.; Lang, C. I.; Hwang, K.; Cuan, G.; Chiang, C.; Bakhru, H.; Olson, R.; Moore, J. A.; Lu, T.-M.; McDonald, J. F. *J. Vac. Sci. Technol. B* **1993** (Sep/Oct), 11 (5), 1825.
- (6) Wu, P. K.; Yang, G.-R.; McDonald, J. F.; Lu, T.-M. *J. Electron. Mater.* **1995**, 24 (1), 53.
- (7) Moore, J. A.; Lang, C.-I.; Lu, T.-M.; Yang, G.-R. *Polym. Mater. Sci. Eng.* **1995**, 72, 437.
- (8) Brown, C. J.; Farthing, A. C. *J. Chem. Soc.* **1953**, 3270.
- (9) Iwamoto, R.; Wunderlich, B. *J. Polym. Sci., Polym. Phys. Ed.* **1973**, 11, 2403.

- (10) Kubo, S.; Wunderlich, B. *Makromol. Chem.* **1972**, 162, 1.
- (11) Isoda, S.; Tsuji, M.; Ohara, M.; Kawaguchi, A.; Katayama, K. *Polymer* **1983**, 24, 1155.
- (12) Kubo, S.; Wunderlich, B. *J. Polym. Sci., Polym. Phys. Ed.* **1972**, 10, 1949.
- (13) Mailyan, K. A.; Pebalk, A. V.; Mishina, E. I.; Kardash, I. E. *Polym. Sci., Ser. A* **1991**, 33 (7), 1530.
- (14) Mailyan, K. A.; Chvalun, S. N.; Pebalk, A. V.; Kardash, I. E. *Polym. Sci., Ser. A* **1992**, 34 (9), 761.
- (15) Mailyan, K. A.; Neverov, V. M.; Pebalk, A. V.; Chvalun, S. N.; Kardash, I. E. *Polym. Sci., Ser. A* **1997**, 39 (5), 809.
- (16) Niegisch, W. D. *J. Appl. Phys.* **1966**, 37, 4041.
- (17) Kubo, S.; Wunderlich, B. *J. Appl. Phys.* **1971**, 42 (12), 4565.
- (18) Kubo, S.; Wunderlich, B. *J. Appl. Phys.* **1971**, 42 (12), 4558.
- (19) Grechkina, E. V.; Sochilin, V. A.; Pebalk, A. V.; Kardash, I. E. *Zh. Org. Khim. (Russian)* **1993**, 29 (10), 1999.
- (20) Alexander, L. E. *X-ray Diffraction Methods in Polymer Science*; Wiley: New York, 1969.
- (21) Bunn, C. W.; Garner, E. V. *Proc. R. Soc. London, Ser. A* **1947**, 189, 39.
- (22) Tadokoro, H.; Seki, S.; Nitta, I.; Yamadera, R. *J. Polym. Sci.* **1958**, 28, 244.
- (23) Kirkpatrick, D. E.; Wunderlich, B. *Makromol. Chem.* **1985**, 186, 2595.

MA981030D